

# Nitrogen-Doped Core-Sheath Carbon Nanotube Array for Highly Stretchable Supercapacitor

Zhitao Zhang, Lie Wang, Yiming Li, Yuhang Wang, Jing Zhang, Guozhen Guan, Zhiyong Pan, Gengfeng Zheng, and Huisheng Peng\*

Supercapacitors as power systems have been attracting extensive attentions for a great potential for various applications, including backup power systems and electric vehicles.<sup>[1–6]</sup> Recently, more attentions are paid to develop stretchable supercapacitors that are playing an increasing role in many new emerging fields, such as portable and integratable electronic equipment, electronic skin, and wearable textile.<sup>[7–11]</sup> However, the electrochemical performance and stretchability of these supercapacitors are far from the expectation for practical applications. A main challenge lies in the difficulty to accurately tune the material composition and structure in electrodes for high properties.<sup>[12,13]</sup> Generally, the electrode of a stretchable supercapacitor can be achieved by depositing the electrically conductive active materials onto the prestrained substrate to form a wrinkled structure.<sup>[11]</sup> However, through this approach the maximal stretched strain cannot be high enough because a high recovery stress may destroy the deposited materials. Another approach is to mix the conductive active material and polymer to prepare composite films.<sup>[14]</sup> Nevertheless, the majority of them is embedded into an elastomeric polymer substrate without making contribution to the electricity and capacitance. Although the performance can be further enhanced by increasing the content of conductive active materials in the resulting composites, the stretchability would be significantly decreased by the increased stiffness.

Here an effective method is developed to fabricate highly stretchable supercapacitors with high electrochemical performances by incorporating a family of nitrogen (N)-doped core-sheath carbon nanotube (NCNT) array as an elastic electrode. The supercapacitors demonstrate a high specific capacitance of  $31.1 \text{ mF cm}^{-2}$ . The specific capacitance has been maintained by 98.9% after stretching to a strain of 400% and by 96% after stretching for 1000 cycles at a strain of 200%.

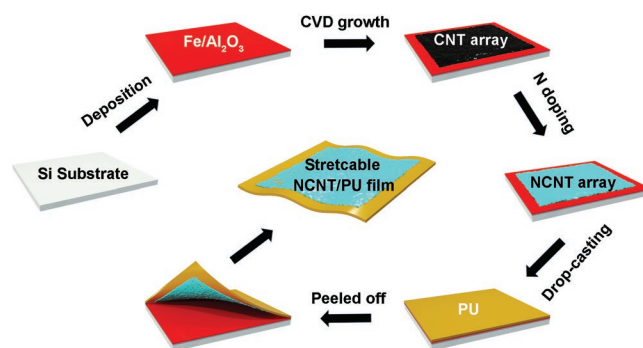
**Figure 1** (see Figure S1, Supporting Information) demonstrates the fabrication of a highly stretchable supercapacitor. A carbon nanotube (CNT) array was first synthesized from ethylene at  $740 \text{ }^\circ\text{C}$  by chemical vapor deposition.<sup>[15,16]</sup> The CNTs were then coaxially re-grown with N-doped layers from acetonitrile also by chemical vapor deposition but at a higher temperature of  $1060 \text{ }^\circ\text{C}$ .<sup>[17–20]</sup> Polyurethane (PU) was coated onto the resulting NCNT array to prepare an NCNT/PU film, followed by deposition of polyvinyl alcohol (PVA) gel electrolyte. Two NCNT/PU films were attached face to face with the PVA gel electrolyte sandwiched between them to produce the desired supercapacitor.

Figure S2 in the Supporting Information shows a scanning electron microscopy (SEM) image of the original CNT array, and the CNTs are highly aligned but also interconnected with each other. Moreover, the aligned and interconnected structure was well maintained after re-growing N-doped layers outside of the CNTs (**Figure 2a–d**), which is critical for the high mechanical and electrical properties described later.

The diameters of NCNTs were controlled by adjusting the re-growing time and traced by transmission electron microscope (TEM) (**Figure 2e–h**; **Figure S3**, Supporting Information). They were gradually increased from  $\approx 11, 16, 28,$  and  $36$  to  $55 \text{ nm}$  with the increasing re-growing time from  $0, 10, 15,$  and  $20$  to  $40 \text{ min}$ , respectively. The new-grown N-doped layers were closely wrapped on the original CNT templates, producing complete NCNTs (**Figure 2i–l**). The re-grown N-doped layer was less uniform than the original CNT, mainly because of the introduction of defects during doping (**Figure S4**, Supporting Information). Meanwhile, this N-doped layer can also grow outside of the CNT bundle (**Figure S5**, Supporting Information). Here, the growth process of NCNT is preceded by depositing

Z. Zhang, L. Wang, Y. Li, J. Zhang, Dr. G. Guan,  
Z. Pan, Prof. H. Peng  
State Key Laboratory of Molecular  
Engineering of Polymers  
Department of Macromolecular Science  
and Laboratory of Advanced Materials  
Fudan University  
Shanghai 200438, China  
E-mail: penghs@fudan.edu.cn

Y. Wang, Prof. G. Zheng  
Department of Chemistry  
Laboratory of Advanced Materials  
Collaborative Innovation Center of Chemistry for Energy Materials  
Fudan University  
Shanghai 200433, China



**Figure 1.** Schematic illustration to the preparation of an elastic NCNT/PU film.

DOI: 10.1002/aenm.201601814

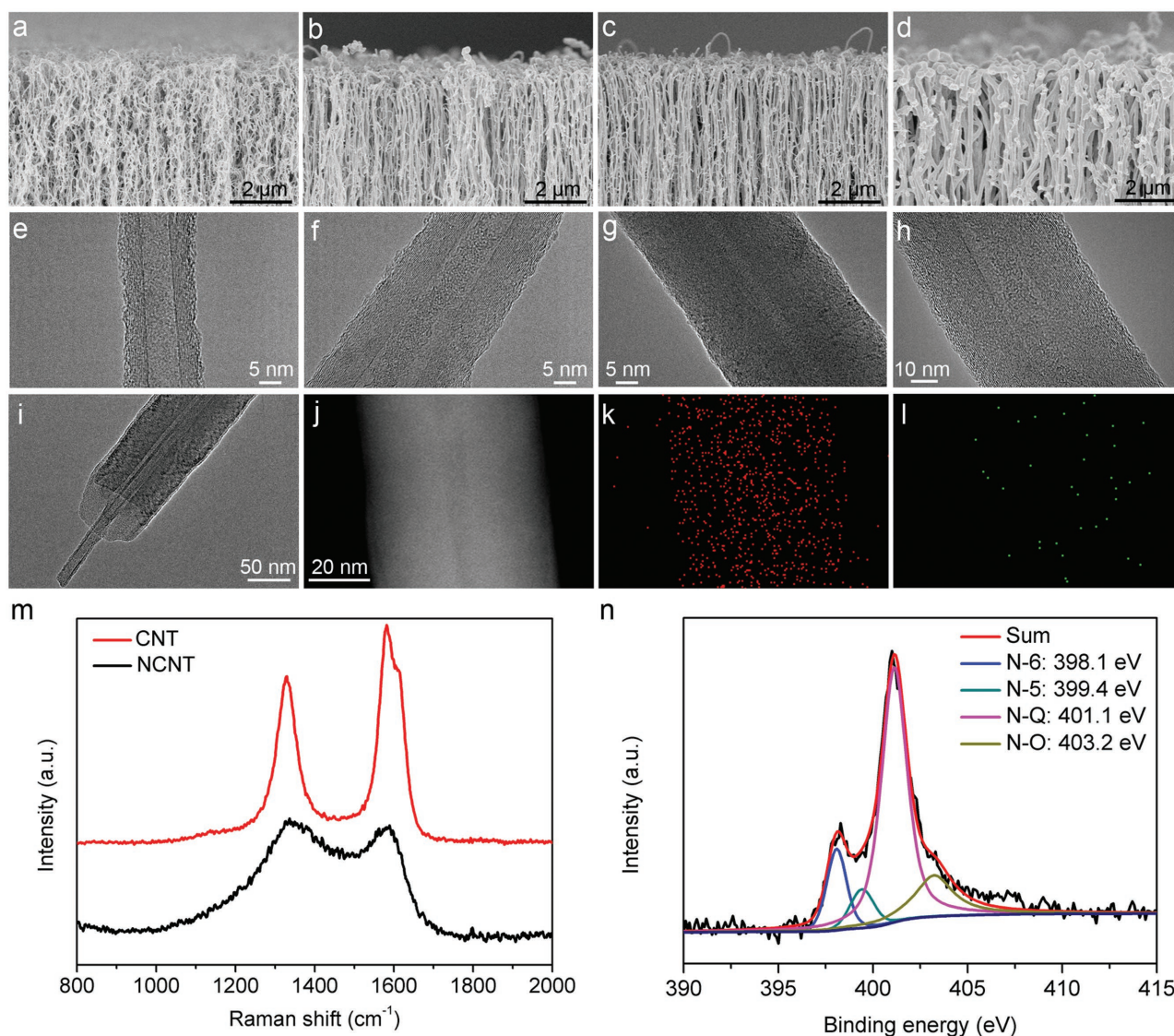


**Figure 2.** a–d) SEM images of NCNT re-grown for a) 10 min, b) 15 min, c) 20 min, and d) 40 min. e–h) TEM images of NCNTs re-grown for e) 10 min, f) 15 min, g) 20 min, and h) 40 min. i) TEM image of NCNT re-grown at 20 min. j) TEM image of NCNT re-grown at 40 min. k, l) Energy-dispersive X-ray spectroscopy images of the NCNT array (j) with the dispersion of k) C and l) N elements. m) Raman spectra of CNT and NCNT re-grown for 20 min. n) N 1s XPS spectra of the NCNT.

the pyrolytic carbon and nitrogen atoms onto the original CNT template.<sup>[17–20]</sup> The change of the chemical structure was characterized by Raman spectra (Figure 2m). The intensity ratio of the D to G bands ( $I_D/I_G$ ) indicates the degree of disorder and defects in carbon systems. The  $I_D/I_G$  ratios of CNT and NCNT were 0.83 and 1.07, respectively. This result proves that the NCNT possesses more defects or disorders than the pristine CNT, which is attributed to the re-grown N-doped layers.<sup>[21]</sup> The X-ray photoelectron spectroscopy (XPS) was further exploited to analyze the types of N-containing species contained in NCNT. According to the XPS N1s spectrum (Figure 2n), N atoms were mainly presented in four forms: pyridine (N-6, 398.1 eV), pyrrole (N-5, 399.4 eV), quaternary (N-Q: 401.1 eV) and pyridine-N-oxide (N-O: 403.2 eV).<sup>[21,22]</sup> The weight percentage of nitrogen in the NCNT was nearly 5.4% at a reaction time of

20 min (Figure S6, Supporting Information). These plentiful N-containing species are beneficial to enhance the surface wettability of NCNT array for the accessibility of gel electrolyte and transport of ions, and provide chemically active sites to introduce pseudocapacitance.<sup>[23–25]</sup>

Figure S7a,b in the Supporting Information further display SEM images of a highly stretchable NCNT/PU film. PU was used as the elastic polymer substrate as it can easily infiltrate into the NCNTs, which was important for realizing a high stretchability (Figure 3a). Here PU was mainly distributed at the bottom of the NCNT/PU film. Note that the thickness of PU can be controlled by varying infiltration conditions without affecting the electrochemical performances of resulting supercapacitors. After coat with the PVA electrolyte, the surface of the NCNT/PU film was uniform (Figure S7c, Supporting

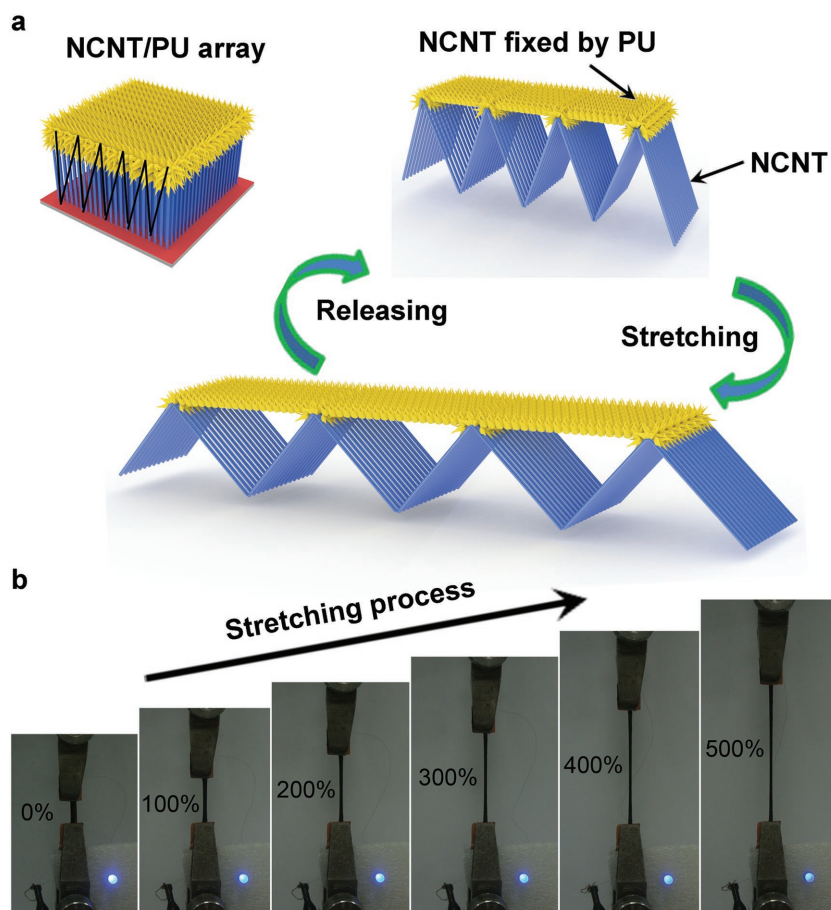


**Figure 3.** a) Schematic illustration to the stretching mechanism of NCNT/PU film. b) Photograph of the NCNT/PU film with strain increased from 0 to 500%.

Information), so the two composite films could be closely contacted with a uniform thickness and high stability under deformation (Figure S7d, Supporting Information). Here the PVA with a high molecular weight was employed as the component of electrolyte to promise the high stretchability, which can be stretched as high as 400% (Figure S8, Supporting Information).<sup>[26]</sup>

The resulting NCNT/PU film was flexible and stretchable without obvious damages during and after bending or stretching (Figures S9 and S10, Supporting Information). Quantitative characterizations were further made by tracing the change of electrical resistance. As expected, the resistance remained almost unchanged under bending (Figure S11, Supporting Information). The resistance changes of NCNT/PU films with different re-growing times at the second synthetic step (or diameters of NCNTs) were also compared under stretching to a strain of 500% (Figures S12 and S13, Supporting Information). When the re-growing time was below 20 min, the resistances were gradually increased with the increasing strain from 0 to 500%. They were 0.98, 1.35, and 1.38  $\text{k}\Omega \text{ cm}^{-1}$  at a strain of 500% at re-growing times of 5, 15, and 20 min, respectively. With the further increase to 40 min, the electrical resistance was sharply increased to 8.30  $\text{k}\Omega \text{ cm}^{-1}$  at a 500% strain.

This phenomenon can be attributed to the fact that it became more difficult for the PU to infiltrate into the smaller voids among NCNTs at the re-growing time beyond 20 min. As a result, PU cannot be effectively interconnected with CNT bundles, resulting in a low stretchability. Therefore, the NCNT/PU film with the re-growing time below 20 min displayed a good stretchability. As a demonstration, we further investigated the electrical resistance of the NCNT/PU film with the re-growing time of 20 min after stretching for 1000 cycles at a strain of 200%, and it was increased by below 6% (Figure S14, Supporting Information). As a demonstration in application, a ribbon-type NCNT/PU composite served as a conducting wire and was connected with a light emitting diode, and its brightness remained almost unchanged during stretching (Figure 3b).

The NCNT arrays with different re-growing times were compared for the use in supercapacitor and studied by galvanostatic charge-discharge curves at 0.1  $\text{mA cm}^{-2}$ . As shown in Figure 4a (see Figure S15, Supporting Information), the specific capacitances in the resulting supercapacitors were increased from 0.38, 18.4, and 21.4 to 31.1  $\text{mF cm}^{-2}$  with increasing re-growing times from 0, 10, and 15 to 20 min, respectively. The increasing specific capacitances were mainly attributed to the following three factors. First, the introduction of N-containing species can remarkably enhance the specific capacitance by providing pseudocapacitance.<sup>[23–25]</sup> Second, the

re-growing N-doped layers can enhance the wettability in the PVA electrolyte and contribute to the capacitance. Thirdly, for the original CNT array, when the PU solution was infiltrated to prepare the CNT/PU film, the perpendicularly aligned CNTs were randomly flattened down on the substrate (Figure S16, Supporting Information). On the contrary, the NCNTs after re-growing the N-doped layers became more crosslinked and stable and thus can maintain the aligned structure after coat of the PU solution (Figure S7a,b, Supporting Information), which ensured the high contact between NCNTs and PVA electrolyte as well as the rapid charge transfer along the aligned direction of NCNTs.<sup>[27]</sup>

However, with the further increase to 40 min, they were reduced to 1.92  $\text{mF cm}^{-2}$  mainly due to the much increased electrical resistance from the resulting NCNT/PU composite electrode under stretching (note that each NCNT/PU film was prestretched during preparation to ensure the subsequent stable and reproducible change of electrical resistance). This result can be further verified by the electrochemical impedance spectroscopy simulation (Figures S17 and S18, Supporting Information). At shorter re-growing time, the internal electrical resistance of the supercapacitor was remarkably decreased, while a dramatic increase in the internal electrical resistance was generated at a re-growing time of 40 min. Therefore, the

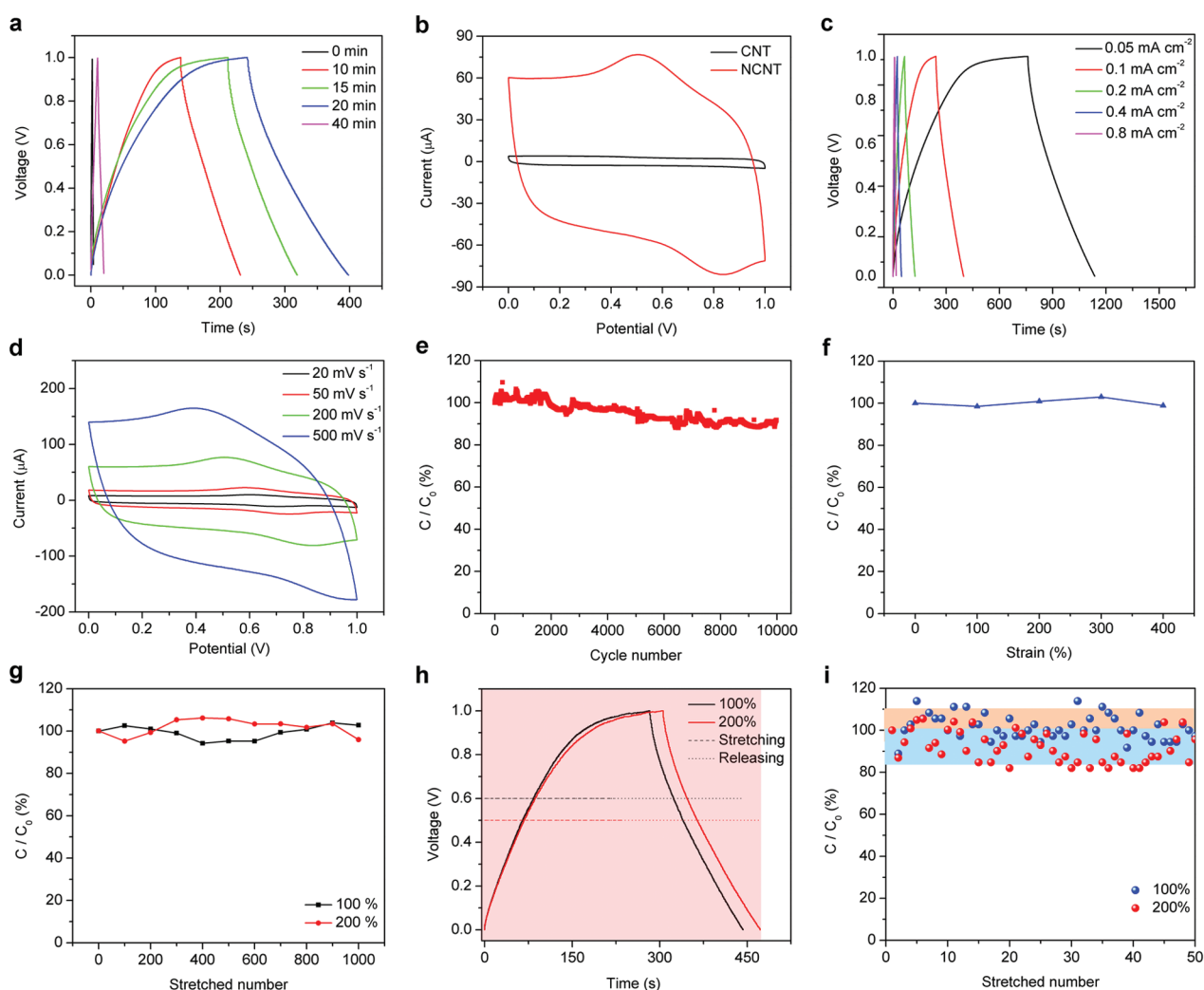


**Figure 4.** a) Galvanostatic charge–discharge curves of the highly stretchable supercapacitors with different re-growth times. The measurements were carried out at a current density of  $0.1 \text{ mA cm}^{-2}$ . b) Cyclic voltammograms of the highly stretchable supercapacitors before and after re-growth for 20 min at a scan rate of  $200 \text{ mV s}^{-1}$ . c) Galvanostatic charge–discharge profiles at increasing current densities. d) Cyclic voltammograms with increasing scan rates. e) Dependence of specific capacitance on cycle number at a current density of  $0.1 \text{ mA cm}^{-2}$ . f) Dependence of specific capacitance on strain. g) Dependence of specific capacitance on stretched cycle number.  $C_0$  and  $C$  correspond to specific capacitances before and after stretching, respectively. h) The galvanostatic charge–discharge curves of supercapacitor under stretching and releasing at a speed of  $5 \text{ mm s}^{-1}$  and current density of  $0.1 \text{ mA cm}^{-2}$ . i) Dependence of specific capacitance of supercapacitor on stretching and releasing number at a current density of  $2 \text{ mA cm}^{-2}$ .  $C_0$  and  $C$  correspond to specific capacitances before and after stretching, respectively.

re-growth time of 20 min was carried out in the following study unless specified otherwise. The specific capacitance was enhanced by over 80 times compared with the original CNT array (Figure 4b)

The rate performance of the supercapacitor is presented in Figure 4c. The specific capacitances were gradually decreased from 37.6, 31.1, 23.6, and 18.6 to  $14.2 \text{ mF cm}^{-2}$  with increasing current densities from 0.05, 0.1, 0.2, and 0.4 to  $0.8 \text{ mA cm}^{-2}$  (Figure S19, Supporting Information), respectively. Cyclic voltammograms were also compared with increasing scan rates of 20, 50, and 200 to  $500 \text{ mV s}^{-1}$ . The similar shapes indicate a good rate performance (Figure 4d). The columbic efficiency of supercapacitor was 90.8% at  $0.1 \text{ mA cm}^{-2}$ . The energy and power densities of the supercapacitor were  $2.16 \text{ } \mu\text{W h cm}^{-2}$

and  $0.05 \text{ mW cm}^{-2}$ , respectively. The electrochemical stability was further verified by cyclic galvanostatic charge–discharge characterizations at  $0.1 \text{ mA cm}^{-2}$ . The specific capacitance was maintained by 91.6% after 10 000 cycles (Figure 4e). Figure 4f compares the specific capacitance before and after stretching to 400%, and it was maintained by 98.9% (Figure S20, Supporting Information). This stable electrochemical performance was attributed to the nearly unchanged electrical resistance of NCNT/PU film in the aligned direction of NCNTs, allowing for the rapid charge transfer and the enlarged contact between NCNT and PVA electrolyte during stretching, although the electrical resistance along the stretching direction was slightly increased.

As expected, this supercapacitor demonstrated a high flexibility with the specific capacitance maintained by 97.5% after

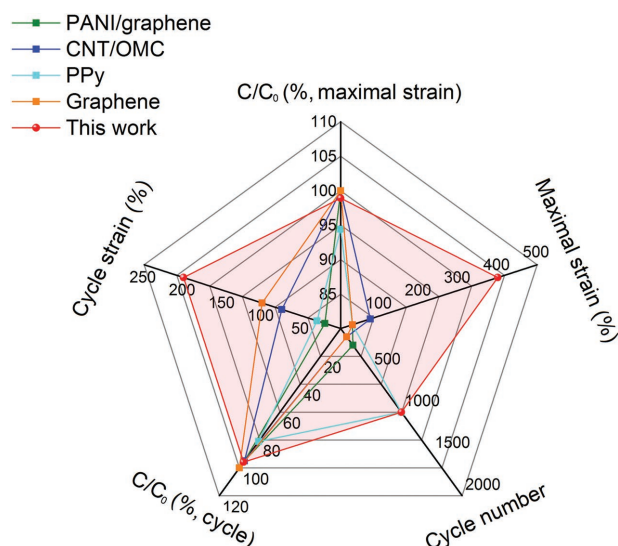


**Figure 5.** Comparison of this highly stretchable supercapacitor with reported supercapacitors in concern of stretchability and stretching cyclic stability. PANI: polyaniline; OMC: ordered mesoporous carbon; PPy: polypyrrole; PEDOT: poly(3,4-ethylenedioxythiophene).  $C_0$  and  $C$  correspond to the specific capacitances before and after stretching, respectively.

bending at a curvature of radius of 1 mm for 1000 cycles (Figure S21, Supporting Information). Meanwhile, the specific capacitance retained 96% after stretching for 1000 cycles at a strain of 200% (Figure 4g), with the interface structure between PVA electrolyte and NCNT/PU film remained nearly unchanged (Figure S22, Supporting Information). The electrochemical property was further traced by dynamically stretching. Figure 4h demonstrates the galvanostatic charge–discharge curves of a supercapacitor during stretching and releasing at a speed of  $5 \text{ mm s}^{-1}$  at a current density of  $0.1 \text{ mA cm}^{-2}$ , indicating an excellent stability of electrochemical performance. The dependence of specific capacitance on stretching and releasing number at a current density of  $2 \text{ mA cm}^{-2}$  were also investigated with the variation below 20% in 50 cycles (Figure 4i). The stretchability and stretching cyclic stability of the supercapacitors are further compared in Figure 5,<sup>[10,11,13,26,28–31]</sup> and our supercapacitors exhibit the highest strain with a stable electrochemical performance.

In summary, aligned N-doped core-sheath CNTs in an array are synthesized for highly stretchable supercapacitors with high electrochemical performances. They display a specific capacitance of  $30.8 \text{ mF cm}^{-2}$  with the strain up to 400%; the specific capacitance can be maintained by 96% after stretching for 1000 cycles. The designed 3D cross-linked structure of the NCNT contributes to both high electrochemical property and stretchability. This work also provides a general and effective strategy in developing the other stretchable electronic devices.

## Experimental Section

A CNT array was first synthesized from ethylene at  $740 \text{ }^\circ\text{C}$  via a chemical vapor deposition process with CNTs perpendicularly growing onto the catalyst-coated silicon wafer with an average height of  $\approx 220 \text{ }\mu\text{m}$ .<sup>[15]</sup> The synthetic details are described in the Supporting Information. The

resulting CNT array was transferred into a tube furnace. The CNT array was then re-grown with N-doped layers outside of the original CNTs also by chemical vapor deposition but with a higher temperature of  $1060 \text{ }^\circ\text{C}$ . Acetonitrile served as both carbon and nitrogen sources, and a mixed gas of argon ( $110 \text{ cm}^3 \text{ min}^{-1}$ ) and hydrogen ( $10 \text{ cm}^3 \text{ min}^{-1}$ ) was used as the carrier gas. The PU solution was directly drop-cast into the NCNT arrays, followed by evaporating the solvent of *N,N*-dimethylformamide and peeling off the resulted NCNT/PU film from the underlying silicon substrate. Finally, an NCNT/PU film was coated with PVA gel electrolyte, and two NCNT/PU composite films were attached to produce a supercapacitor. Here the weights of NCNT/PU composite film electrodes ( $0.2 \times 0.3 \text{ cm}$ ) used for constructing the supercapacitor were increased from 0.748, 0.805, 0.891, and 0.919 to 0.993 mg with increasing re-growing time from 0, 10, 15, and 20 to 40 min, respectively. The PVA gel electrolyte was prepared by adding  $\text{H}_3\text{PO}_4$  into PVA aqueous solution with the PVA/ $\text{H}_3\text{PO}_4$  weight ratio of 1/1.5.<sup>[25]</sup>

## Supporting Information

Supporting Information is available from the Wiley Online Library or from the author.

## Acknowledgements

This work was supported by NSFC (21225417, 51573027, 51403038), STCSM (15XD1500400, 15JC1490200) and the Program for Outstanding Young Scholars from Organization Department of the CPC Central Committee.

Received: August 18, 2016

Revised: September 16, 2016

Published online: November 8, 2016

- [1] X. Yang, K. Shi, I. Zhitomirsky, E. D. Cranston, *Adv. Mater.* **2015**, *27*, 6104.
- [2] Z. Niu, W. Zhou, X. Chen, J. Chen, S. Xie, *Adv. Mater.* **2015**, *27*, 6002.
- [3] M. F. El-Kady, V. Strong, S. Dubin, R. B. Kaner, *Science* **2012**, *335*, 1326.
- [4] P. Simon, Y. Gogotsi, *Nat. Mater.* **2008**, *7*, 845.
- [5] Y. Zhao, J. Liu, Y. Hu, H. Cheng, C. Hu, C. Jiang, L. Jiang, A. Cao, L. Qu, *Adv. Mater.* **2013**, *25*, 591.
- [6] J. Jiang, Y. Li, J. Liu, X. Huang, C. Yuan, X. W. D. Lou, *Adv. Mater.* **2012**, *24*, 5166.
- [7] J. Zhu, L. Cao, Y. Wu, Y. Gong, Z. Liu, H. E. Hoster, Y. Zhang, S. Zhang, S. Yang, Q. Yan, P. M. Ajayan, R. Vajtai, *Nano Lett.* **2013**, *13*, 5408.
- [8] X. Lang, A. Hirata, T. Fujita, M. Chen, *Nat. Nanotechnol.* **2011**, *6*, 232.
- [9] D. Kim, G. Shin, Y. J. Kang, W. Kim, J. S. Ha, *ACS Nano* **2013**, *7*, 7975.
- [10] Y. Xie, Y. Liu, Y. Zhao, Y. H. Tsang, S. P. Lau, H. Huang, Y. Chai, *J. Mater. Chem. A* **2014**, *2*, 9142.
- [11] Z. Niu, H. Dong, B. Zhu, J. Li, H. H. Hng, W. Zhou, X. Chen, S. Xie, *Adv. Mater.* **2013**, *25*, 1058.
- [12] T. Chen, Y. Xue, A. K. Roy, L. Dai, *ACS Nano* **2014**, *8*, 1039.
- [13] Z. Yang, J. Deng, X. Chen, J. Ren, H. Peng, *Angew. Chem. Int. Ed.* **2013**, *52*, 13453.
- [14] M. Yu, Y. Zhang, Y. Zeng, M.-S. Balogun, K. Mai, Z. Zhang, X. Lu, Y. Tong, *Adv. Mater.* **2014**, *26*, 4724.
- [15] Z. Zhang, K. Guo, Y. Li, X. Li, G. Guan, H. Li, Y. Luo, F. Zhao, Q. Zhang, B. Wei, *Nat. Photonics* **2015**, *9*, 233.
- [16] M. K. Shin, J. Oh, M. Lima, M. E. Kozlov, S. J. Kim, R. H. Baughman, *Adv. Mater.* **2010**, *22*, 2663.
- [17] W. Xu, T. Kyotani, B. K. Pradhan, T. Nakajima, A. Tomita, *Adv. Mater.* **2003**, *15*, 1087.

- [18] Q.-H. Yang, P.-X. Hou, M. Unno, S. Yamauchi, R. Saito, T. Kyotani, *Nano Lett.* **2005**, *5*, 2465.
- [19] Z. Pan, J. Ren, G. Guan, X. Fang, B. Wang, S.-G. Doo, I. H. Son, X. Huang, H. Peng, *Adv. Energy Mater.* **2016**, *6*, 1600271.
- [20] J. Lim, U. N. Maiti, N.-Y. Kim, R. Narayan, W. J. Lee, D. S. Choi, Y. Oh, J. M. Lee, G. Y. Lee, S. H. Kang, H. Kim, Y.-H. Kim, S. O. Kim, *Nat. Commun.* **2016**, *7*, 10364.
- [21] F. M. Hassan, V. Chabot, J. Li, B. K. Kim, L. Ricardez-Sandoval, A. Yu, *J. Mater. Chem. A* **2013**, *1*, 2904.
- [22] P. Chen, J.-J. Yang, S.-S. Li, Z. Wang, T.-Y. Xiao, Y.-H. Qian, S.-H. Yu, *Nano Energy* **2013**, *2*, 249.
- [23] L.-F. Chen, Z.-H. Huang, H.-W. Liang, Q.-F. Guan, S.-H. Yu, *Adv. Mater.* **2013**, *25*, 4746.
- [24] Z. Wen, X. Wang, S. Mao, Z. Bo, H. Kim, S. Cui, G. Lu, X. Feng, J. Chen, *Adv. Mater.* **2012**, *24*, 5610.
- [25] H. M. Jeong, J. W. Lee, W. H. Shin, Y. J. Choi, H. J. Shin, J. K. Kang, J. W. Choi, *Nano Lett.* **2011**, *11*, 2472.
- [26] C. Zhao, C. Wang, Z. Yue, K. Shu, G. G. Wallace, *ACS Appl. Mater. Interfaces* **2013**, *5*, 9008.
- [27] H. Peng, X. Sun, F. Cai, X. Chen, Y. Zhu, G. Liao, D. Chen, Q. Li, Y. Lu, Y. Zhu, *Nat. Nanotechnol.* **2009**, *4*, 738.
- [28] P. Xu, B. Wei, Z. Cao, J. Zheng, K. Gong, F. Li, J. Yu, Q. Li, W. Lu, J.-H. Byun, B.-S. Kim, Y. Yan, T.-W. Chou, *ACS Nano* **2015**, *9*, 6088.
- [29] X. Zang, M. Zhu, X. Li, X. Li, Z. Zhen, J. Lao, K. Wang, F. Kang, B. Wei, H. Zhu, *Nano Energy* **2015**, *15*, 83.
- [30] T. G. Yun, B. i. Hwang, D. Kim, S. Hyun, S. M. Han, *ACS Appl. Mater. Interfaces* **2015**, *7*, 9228.
- [31] N. Zhang, W. Zhou, Q. Zhang, P. Luan, L. Cai, F. Yang, X. Zhang, Q. Fan, W. Zhou, Z. Xiao, X. Gu, H. Chen, K. Li, S. Xiao, Y. Wang, H. Liu, S. Xie, *Nanoscale* **2015**, *7*, 12492.